Biol. Cybern. 48, 213–222 (1983)

Biological Cybernetics

Model Emulates Human Smooth Pursuit System Producing Zero-Latency Target Tracking

A. Terry Bahill and Jack D. McDonald*

Biomedical Engineering Program, Carnegie-Mellon University, Pittsburgh, PA, USA

Abstract. Humans can overcome the 150 ms time delay of the smooth pursuit eye movement system and track smoothly moving visual targets with zero-latency. Our target-selective adaptive control model can also overcome an inherent time delay and produce zero-latency tracking. No other model or man-made system can do this. Our model is physically realizable and physiologically realistic. The technique used in our model should be useful for analyzing other time-delay systems, such as man-machine systems and robots.

1 Introduction

Experiments with transient target waveforms have shown that there is a time delay of about 150 ms in the human smooth pursuit eye movement system (Rashbass, 1961). For example, when a target starts to move there is a 150 ms delay before the eye starts to move, as shown in Fig. 1. When the target stops there is a 150 ms delay before the eye stops (Fig. 1). However, when a human (or a monkey) tracks a target that is moving sinusoidally, the subject quickly locks on to the target and tracks with neither latency nor phase lag. It is as if the subject creates an internal model of the target movement and uses this model to help track the target. This internal model has variously been called a predictor (Westheimer, 1954; Stark et al., 1962), a long term learning process (Dallos and Jones, 1963), a percept tracker (Yasui and Young, 1975; Young, 1977; Steinbach, 1976; Mack et al., 1982), a neutral motor pattern generator (Eckmiller, 1981), and a target-selective adaptive controller (McDonald and Bahill, 1983). To help explain how the human performs such zero-latency tracking, we developed a model that does the same. This paper explains our model. The two essential capabilities of our model are the ability to predict future values of target velocity, and the ability to compensate for system dynamics.

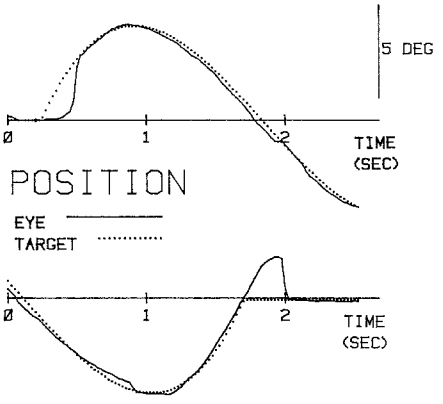

Fig. 1. Typical beginning (top) and ending (bottom) of human tracking. The target position (dotted line) and eye position (solid line) are plotted as functions of time. The time axis is labeled in seconds. This figure shows that the latency of the smooth pursuit system is less than that of the saccadic system. Smooth pursuit eye movements began 150 ms after the target began and the saccade occured 200 ms after the beginning. Smooth pursuit velocity began to fall 125 ms after the target stopped and the saccade occured 250 ms after the ending. Rightward movements are upward deflections. The target was moving $\pm 5°$ from primary position. The mean squared error between the target position and the eye position (pmse) was 0.3 deg^2 for the top 0.4 deg^2 for the bottom record

The target-selective adaptive control (TSAC) model can overcome an inherent time delay and produce zero-latency tracking of predictable targets. We know of no other physically realizable model or man-made system that can do this. Previous studies of the predictive capabilities of the smooth pursuit eye movement system have been analysis only (Westheimer, 1954; Stark et al., 1962; Dallos and Jones, 1963; Michael and Melvile Jones, 1966; Steinbach, 1976; Lanman et al., 1978; Winterson and Steinman, 1978; Schalen, 1980; Eckmiller, 1981), have produced physi-

* Present address: The Mitre Corporation, Bedford, MA, USA

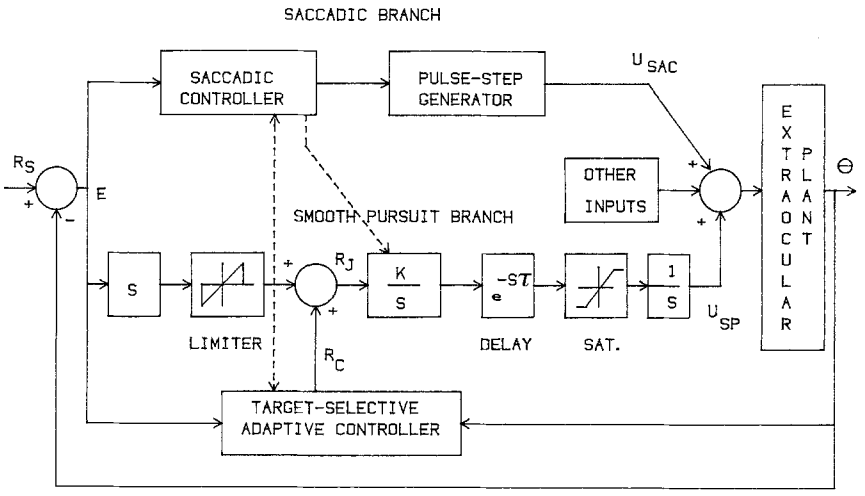

Fig. 2. The Target-Selective Adaptive Control (TSAC) model for the human eye movement system

cally unrealizable models (Dallos and Jones, 1963), or have produced models that did not track the target with zero-latency (Greene and Ward, 1979; Yasui and Young, 1975). Among physiological time-delay systems only the saccadic and smooth pursuit eye movement systems exhibit zero-latency tracking; manual tracking systems (McRuer, 1980; Kleinman et al., 1980) and even the vergence eye movement system fail to show prediction (Rashbass, 1981). Similarly, in the control engineering literature we found no systems that could overcome time delays and track signals with zero-latency (McDonald and Bahill, 1983). Therefore, our model for this system is unique. No other models produce zero-latency tracking by time-delay systems.

1.1 Relationship of Present Model to Previous Models

The Target-Selective Adaptive Control (TSAC) model (Fig. 2) has the three major branches: the saccadic branch, the smooth pursuit branch, and the target-selective adaptive controller. The adaptive controller is the topic of this paper. The exact details of the other boxes in this model are unimportant for the purpose of this paper, which is to explain how the target-selective adaptive controller produces zero-latency tracking of predictably moving targets. Therefore, we will only briefly discuss these other boxes.

First, we had to select a model for the extraocular plant. The sixth-order linear homeomorphic model (Bahill et al., 1980) that we initially used provided accuracy for the fine details of saccadic eye movements. However, we soon discovered that simpler models worked just as well for smooth pursuit eye movements. For these slow movements it was sufficient, and more computationally efficient, to use a second-order plant (Westheimer, 1954; Zuber et al., 1968). In fact, when we compared the outputs generated by the second-order and the sixth-order plants, we found no differences in either smooth pursuit or adaptation.

Many models have been proposed for the saccadic branch including a control systems sampled-data model (Young and Stark, 1963; Young, 1981), a neurophysiological analog (Robinson, 1975; Van Gisbergen et al., 1981), and a block diagram intermediate (Becker and Jurgens, 1979). However, for the TSAC model, we chose a simplified saccadic branch, because the details of saccade generation are not important, only the existence of saccades is important. The saccadic branch contains two nonlinear, but simple, elements: the controller and the generator. The saccadic controller monitors the error between target and eye position. When the error exceeds a preset threshold, the controller – after a time delay of 150 ms – sends a command to the saccadic generator. The values for the error threshold and the time delay, were matched to our human data. Although, the error thresholds and time delays varied for individual subjects and different conditions, we found 0.5° and 150 ms to be common. So for the model we set the error threshold to 0.5° when the adaptive controller is turned off and 0.3° when the adaptive controller is turned on. The saccadic generator converts the saccade command into the required extraocular plant input signal. The input for the second-order plant is a step. The input for the sixth-order linear homeomorphic model is a pulse-step.

The smooth pursuit branch is similar to that presented by Young and Stark (1963). Once again a very simple model was chosen. This model was sufficient for explaining how the target-selective adaptive controller produces zero-latency tracking of predictably moving targets.

The differentiator in the smooth pursuit branch of Fig. 2 changes position into velocity. The limiter in the

smooth pursuit branch prevents a response to an input greater than $\pm 70°/s$, which is compatible with human behavior (Schalen, 1980). Different values for this limit have been suggested. However, the exact value of this parameter is unimportant, because humans only attain zero-latency tracking of slowly moving targets.

The control loop integrator in the smooth pursuit branch was suggested by two experimental results. First, humans can track ramps with zero steady-state error (Rashbass, 1961). This implies the existence of at least one integrator. Second, open-loop experiments have demonstrated that the frequency response of the smooth pursuit branch has a slope of -23 dB per decade (Wyatt and Pola, 1979). This can be approximated with an integrator. The gain K of the smooth pursuit branch has been estimated from open-loop experiments to be between 2 and 5 (Young, 1971; Mack et al., 1982). Originally we used a gain of 4 and a pure integrator in the forward path of the pursuit branch. However, this combination yielded a closed-loop time constant of 250 ms, and our start-up transient data (Fig. 1) indicated that this time constant should be smaller. Therefore, we have recently replaced the pure integrator (K/s in Fig. 2) with a leaky integrator $K/(\tau_2 s+1)$ with $K=2$ and $\tau_2=0.15$ s. We are performing experiments to find the best value for τ_2.

In addition to the limiter before the control loop integrator, a saturation element is needed after the control loop integrator to prevent the output from producing velocities greater than the human, i.e. 60°/s. A parabolic target waveform – i.e. one with constantly increasing velocity – demonstrates the need for such a saturation element. For example, in the beginning the eye would track the target with little error. However, after tracking the target for some time the eye might fall behind. The target velocity could be 70°/s, for example, while the eye velocity was 60°/s. Since the retinal slip would be less than the limiter value, the smooth pursuit velocity would continue to increase; this is inconsistent with observed human behavior. The model, therefore, has a saturation element.

The last integrator in the smooth pursuit branch converts the velocity signal to the position signal that is required by the extraocular plant models.

The models of Yasui and Young (1975) and Young (1981) added a corollary discharge pathway to give eye position information to the smooth pursuit system. We have also included a pathway providing eye position information. However in our model this information is processed by the adaptive controller before it is sent to the smooth pursuit branch. Several investigators have suggested that perceived target velocity is the stimulus for the smooth pursuit system. In this context R_J of Fig. 2 represents this perceived velocity.

We have discussed all of the elements of the smooth pursuit branch of our model (Fig. 2). However, we emphasize that the exact details of these boxes are unimportant; that whole branch could be replaced by anyone's model. The important aspect about our model is the target-selective adaptive controller. It is this controller that allows zero-latency tracking. Such a controller could be added to a wide variety of other models or control systems.

2 Experimental Methods

The movements of each eye were measured with a standard photoelectric system (Bahill et al., 1975, 1981; Bahill 1981). Target and eye movements were amplified (0–100 Hz bandwidth), passed through a 12 bit analog to digital converter sampling at 1000 Hz, and stored on a disk in the computer. The linear range for the measurement of horizontal eye movements extended $\pm 10°$ from primary position. Instrumentation noise was less than ten millivolts: it was one thousandth of the full scale range. One minute of arc movements have been recorded with this equipment. Bandwidths for the data shown in this paper were 80 Hz and 4.4 Hz, respectively, for the eye position and eye velocity records.

Target waveforms were generated by an LSI-11 microcomputer. Our most useful waveforms were sinusoidal, parabolic, cubic and a pseudo-random acceleration waveform. They are described in detail by Bahill and McDonald (1983). These waveforms drove a mirror galvanometer that reflected a laser beam, thus projecting a red dot on a curved screen 57 cm in front of the subject. Keeping the target at a fixed distance eliminated vergence eye movements. Our subjects' heads were restrained with a headrest and bite bar to eliminate vestibulo-ocular eye movements.

3 Human Eye Tracking

Humans can learn to track any predictable waveform that is smooth and periodic, provided the target does not exceed certain frequency, velocity and acceleration limits (Bahill and McDonald, 1983). For example, Fig. 3 shows zero-latency tracking of a cubic waveform: the mean square error between target and eye position was 0.04 deg^2. These small mean square errors show not only that our subjects were tracking well, but also that our instrumentation system was reliable: these mean square errors represent the sum of human error, measurement nonlinearities and instrumentation noise. Note also that the eye velocity dots cluster around the target velocity line. This further indicates that the human was tracking the target with the appropriate waveform.

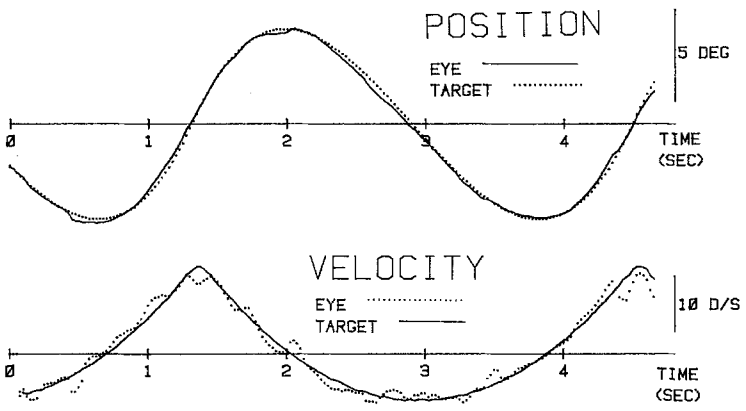

Fig. 3. Human zero-latency tracking of cubic target waveform. The top record shows eye position (solid) and target position (dotted); the bottom record shows target velocity (solid) and eye velocity (dotted). Time axis is labeled in seconds. The pmse was 0.04 deg^2 and the velocity mean squared error (vmse) was 1.7 deg^2/s^2

To estimate the gain K of the smooth pursuit branch of Fig. 2, we performed a series of "open-loop" experiments. In these experiments we made a target movement and waited for the eye to respond. When the eye moved, we used the measured eye position signal to instantaneously move the target by the same amount. Thus the eye movements became ineffective in correcting the retinal error and the feedback loop was in essence opened. In this mode the ratio of target velocity to eye velocity equals the forward-path gain, K, divided by the frequency, s. For sinusoidal target motions, the forward-path gain was between 2 and 5 during the first 500 ms after the loop was opened. After this, strange things happened. Sometimes the gain rose as high as 20. And sometimes there was an amazing absence of saccades although the position error was in excess of 1°. When this occured, the eye movements were larger than the target movements; sometimes the eye movements were symmetric about the target and sometimes they were offset. This off-foveal tracking without saccades has been shown previously in open loop experiments (Wyatt and Pola, 1979; Mack et al., 1982; Leigh et al., 1982). There are several possible explanations for the strange behavior after the first half second. First, although the retinal error is held constant this does not get rid of the effects of the adaptive controller. Second, the subjects may have voluntarily suppressed saccades. Third, the smooth pursuit system is a foveal tracking system, but in these open-loop experiments the target was not on the fovea, therefore, a peripheral tracking system had to be used. Fourth, for large eye movements the instrumentation system was driven into a nonlinear region. Therefore, eye movement turn arounds were caused by the instrumentation nonlinearity and not by the open-loop system. Fifth, the subjects could have noticed the change in target movement and volitionally changed their control strategy. In spite of these difficulties, we found enough good data to suggest that the smooth pursuit forward-path gain is between 2 and 5.

How can humans attain zero-latency tracking of predictable waveforms in spite of the inherent 150 ms time delay? To answer this question we constructed a model that could also overcome the effect of a large time delay and achieve zero-latency tracking of targets moving with predictable trajectories.

4 The TSAC Model

The TSAC model of Fig. 2 has three branches: the saccadic branch that corrects position errors; the smooth pursuit branch that corrects velocity errors; and the target-selective adaptive controller that synthesizes the adaptive signal that allows the smooth pursuit branch to match the target velocity without a time delay.

The target-selective adaptive controller performs three functions: identification, evaluation, and synthesis. The identification function looks at retinal velocity error and eye position, θ. It computes target amplitude, velocity, period, and the time since the last change in direction. When the target changes direction, the parameters are stored, and collection begins in the new direction. It only identifies targets that have smooth waveforms (no velocity discontinuities), and frequencies between 0.1 and 1 Hz. A target with frequency below 0.1 Hz is considered to be stationary. If the target stops for more than 50 ms, or if both position and velocity errors rise above their thresholds (0.3 and 3°/s), then the evaluation function sets the adaptive signal to zero. When the target is identified, an adaptive signal, $r_c(t)$, is synthesized to cause tracking with no time delay or velocity error.

Zero-latency tracking can occur after only one-quarter cycle of target motion. This observation is reflected within the model as a default target identification. This default waveform is used by the adaptive controller when a smoothly moving target is present, but there is not yet sufficient information for identifi-

cation and synthesis. When the default is correct, tracking follows that of the best experienced subjects. When the default is incorrect, tracking is typical of inexperienced subjects.

The various elements of the model interact. The adaptive controller reduces the threshold of the saccadic controller when the position error drops below 0.3° while the velocity error is less than 3°/s; this interaction is represented in Fig. 2 with a dashed line from the adaptive controller to the saccadic controller. The saccadic controller inhibits the evaluation function of the adaptive controller during a saccade; this control signal pathway is shown in Fig. 2 with a dashed line from the saccadic controller to the adaptive controller. During a saccade the saccadic controller also sends a hold command to the smooth pursuit control loop integrator. This command prevents the integrator from responding to the low velocity portions of a saccade; this control signal pathway is shown in Fig. 2, with a dashed line between the saccadic controller and the smooth pursuit integrator.

4.1 The Adaptive Controller

We have developed a general control scheme that allows a system to overcome a time delay and track predictable targets with zero latency (McDonald and Bahill, 1983). In this scheme, the controller must be able to predict future values of the target, and it must know the dynamics of the system. Then it can generate a signal, which when added to the target signal, can make the output equal to the input, which is zero-latency tracking. The smooth pursuit system is a velocity tracking system, so the controller must be able to predict future values of target velocity. For example, if $\dot{r}_s(t)$ is the present velocity, it must produce $\dot{r}_s(t+\tau)$ where τ is the time delay of the smooth pursuit system. Next the controller must modify this equation to compensate for the dynamics of the system. For the model of Fig. 2 this compensation consists of taking a derivative and dividing by K (McDonald and Bahill, 1983). Thus the adaptive signal becomes

$$r_c(t)=\frac{1}{K}\frac{d}{dt}\dot{r}_s(t+\tau). \tag{1}$$

To further illustrate our technique for compensating for system dynamics we note in passing that if we replace the pure integrator (K/s in Fig. 2) with a leaky integrator ($K/\tau_2 s+1$), then the A matrix is $-1/\tau_2$, the b vector is $1/\tau_2$ and the adaptive signal becomes

$$r_c(t)=\frac{1}{K}\left[\frac{d}{dt}\tau_2\dot{r}_s(t+\tau)+\dot{r}_s(t+\tau)\right].$$

The adaptive signal allows the smooth pursuit system to overcome the time delay. To synthesize this signal the adaptive controller must be able to both predict future values of the target velocity, and compute first derivatives. These are reasonable computations for the human brain.

4.2 Two Methods of Predicting Target Velocity

Our model uses two alternative methods for predicting target velocity: menu selection and extrapolation using a difference equation. We are currently working on a third technique using a Kalman filter. The first method has a list, or menu, of the target waveforms that the model has learned to track. Some of the equations on present menu are for sinusoidal, parabolic, and cubic waveforms. These equations are derived as follows. For sinusoidal motion the target velocity is given by

$$\dot{r}_s(t)=A\omega\cos(\omega t) \tag{2}$$

so the adaptive signal, derived by substituting (2) into (1), is

$$r_c(t)=\frac{-A\omega^2}{K}\sin\omega(t+\tau). \tag{3}$$

The computation of $r_c(t)$ requires estimation of the sinusoidal amplitude A and frequency ω, and knowledge of the system gain K and time delay τ. If the controller identifies the target waveform as sinusoidal it will use this equation. On the other hand, if the controller identifies the target waveform as parabolic, then it will use the following parabolic equations.

$$\dot{r}_s(t)=\frac{-32A}{T^2}[t-T/4] \quad \text{for} \quad 0<t<\frac{T}{2}, \tag{4}$$

where A is the amplitude and T is the period of the target. The adaptive signal needed for zero-latency tracking is derived from Eqs. (1) and (4)

$$r_c(t)=\frac{-32A}{KT^2} \quad \text{for} \quad -\tau<t<\frac{T}{2}-\tau. \tag{5}$$

The other half of the period is of identical form but of opposite sign. If the controller identifies the waveform as cubic, then it will select the cubic equations. The velocity of the cubic target waveform is given by

$$\dot{r}_s(t)=\frac{10.39A}{T}[6(t/T)^2-6(t/T)+1] \tag{6}$$

and the adaptive signal is

$$r_c(t)=-10.39\frac{6A}{KT^2}\left[\frac{2(t+\tau)}{T}-1\right]. \tag{7}$$

The menu selection method of synthesizing the adaptive signal r_c selects the correct target equation from

the menu [Eqs. (2), (4), and (6)] and then computes the required adaptive signal. Novel waveforms are tracked poorly until a new equation is added to the menu.

The second method of predicting target velocity uses a second-order difference equation. The compensation for system dynamics is again differentiation and division by K. Therefore, the resulting adaptive signal is

$$r_c([n+1]h) = a\dot{r}_s(nh) - b\dot{r}_s([n-1]h) + c\dot{r}_s([n-2]h) \quad (8)$$

where

$$a = \frac{\tau}{h^2 K} \quad b = \frac{2\tau - h}{h^2 K} \quad c = \frac{\tau - h}{h^2 K}.$$

The element τ is smooth pursuit delay, h is adaptive sampling period (normally 5 ms), n is the index for discrete time, and K is the smooth pursuit forward path again. We performed several simulations to determine if the difference equation predictor, Eq. (8), or the menu selection predictor, Eqs. (3), (5), and (7), produced more human like results.

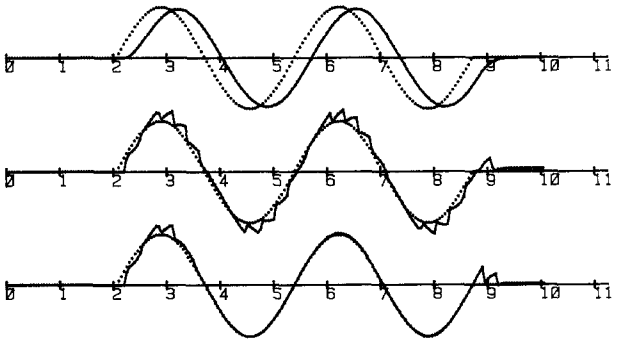

Fig. 4. Position as a function of time for the TSAC model tracking a sinusoidal target. The top axis shows the smooth pursuit branch alone. The middle axis has both the smooth pursuit and the saccadic branches. The bottom axis includes the saccadic branch, the smooth pursuit, and the target-selective adaptive controller

5 Model Results

Each branch of the TSAC model can be turned on and off independently. Figure 4 shows the model (solid line) tracking a sinusoidal target (dotted line) with various branches isolated. For the top record the smooth pursuit branch was turned on, but the saccadic branch and the adaptive controller were turned off. For the middle record the smooth pursuit and saccadic branches were turned on, but the adaptive controller was turned off. For the bottom record all three subsystems were turned on. Only the bottom record resembles normal human tracking.

Now that we had a model, we used it to fine tune the parameter values of the system. Our open-loop experiments suggested that the smooth pursuit forward-path gain (K in Fig. 2) was between 2 and 5. In order to narrow the range for this gain we used the model. Figure 5A shows the model tracking a 0.3 Hz parabolic target waveform with a forward-path gain of 4. Figure 5B, in contrast, shows the end of tracking with a gain K of 2. The lower gain caused the smooth pursuit velocity to decay slower, and produced multiple saccades at the beginning and ending of tracking. The gain of 4 best matches the end of tracking transient from human experimental data. Therefore, we used this value for all subsequent simulations.

The bottom traces in Fig. 5 show the control signals r_J. These control signal are vastly different for our predictor techniques. In Fig. 6 the TSAC model with the difference equation predictor [Eq. (8)] is shown tracking a 0.3 Hz parabolic target waveform. Although the adaptive signal r_J varied widely, the position and velocity tracked the target well.

To learn more about the smooth pursuit system we ran the model in a manner that it was not designed to run in. The effects of selecting the wrong waveform from the model's menu are shown in Fig. 7, where a parabolic adaptive signal, Eq. (3), was used when the

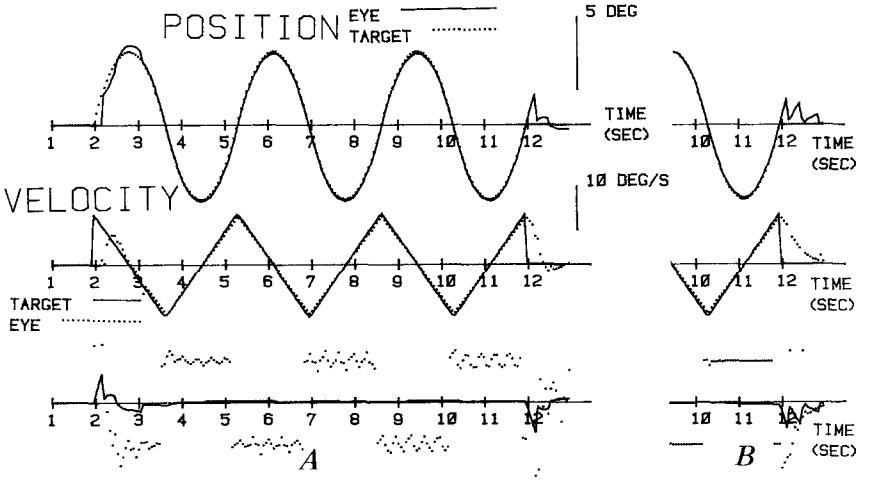

Fig. 5. A TSAC model with menu selection predictor tracking 0.3 Hz parabolic target waveform. Gain, K, was 4. The top axis shows target (dotted) and model (solid) position. Center axis contains graph of target (solid) and eye (dotted) velocities. The bottom axis contains position error (solid) and the signal r_J of Fig. 2 (dotted). The time axis is labeled in seconds. The pmse was 0.09 deg^2, and vmse was 34.9 deg^2/s^2 for the entire record including starting and stoping transients. **B** Termination of tracking after the gain K has been reduced from 4 to 2. For the entire 12 s simulation, the pmse was 0.15 deg^2 and the vmse was 57.4 deg^2/s^2

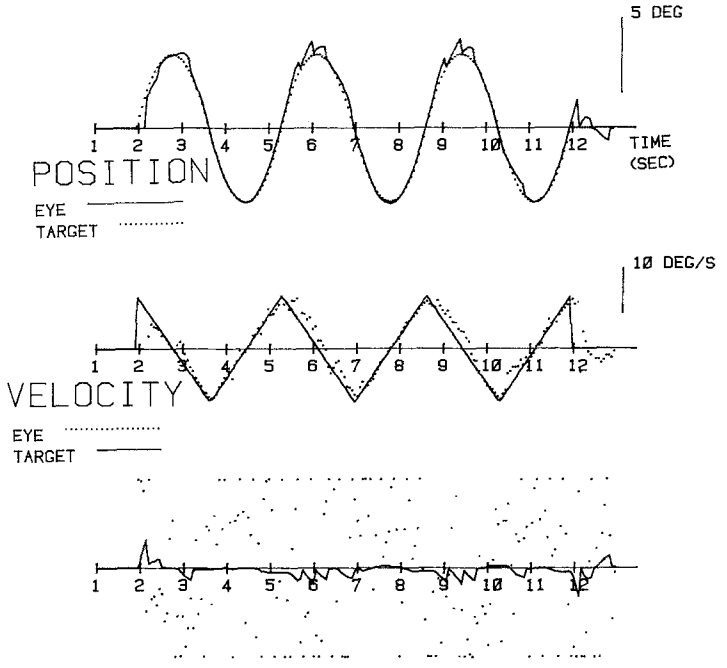

Fig. 6. TSAC model with difference equation predictor tracking parabolic target. The pmse was 0.21 deg^2 and the vmse was 86.4 deg^2/s^2

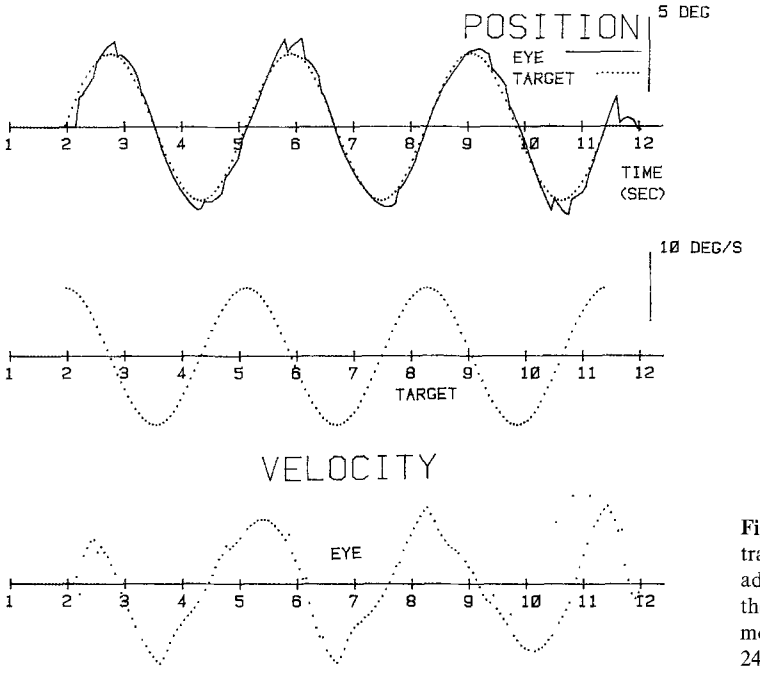

Fig. 7. TSAC model with menu selection predictor tracking sinusoidal target with incorrect (parabolic) adaptive signal. The top trace is target and model position, the middle trace is target velocity, and the bottom trace is model velocity. The pmse was 0.24 deg^2 and the vmse was 24.2 deg^2/s^2

target waveform was sinusoidal. The tracking was zero latency, but the error was large and there were many saccades. Figure 8 shows a human's performance with a large error and many saccades. The human's velocity looks like the velocity of a parabolic waveform, while the target waveform looks sinusoidal. This human tracking suggests a wrong guess. Examples such as these were common for sinusoidal and parabolic target waveforms. However, we did not find such illustrative examples for the cubic waveform.

6 Discussion

6.1 Comparison of the Two Predictor Methods

The TSAC model emulates the human; it can achieve zero-latency tracking of predictably moving targets. In this model we used two alternative methods of predicting target velocity. Both of these methods enabled the model to track sinusoidal, parabolic, and cubic waveforms. The difference equation predictor [Eq. (8)] provides only an approximation to the equations of

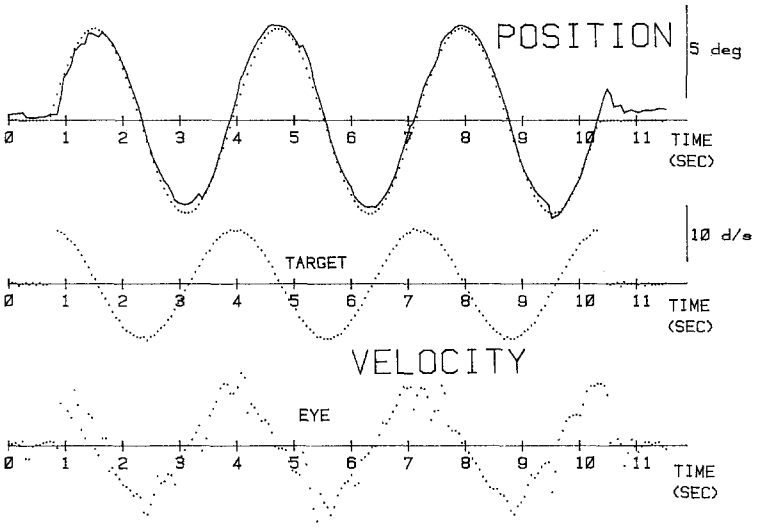

Fig. 8. Human tracking sinusoidal target waveform. The top trace shows target position (dotted) and eye position (solid), the middle trace shows target velocity, and the bottom trace shows eye velocity. The eye velocity waveform does not match the target velocity waveform. The pmse was 0.18 deg^2 and the vmse was 5.8 deg^2/s^2

Table 1. Position and velocity mean square errors for sinusoidal tracking by experienced humans and by the TSAC model with the menu selection and difference equation predictors

Frequency (Hz)	Human		Menu selection		Difference equation	
	pmse	vmse	pmse (deg^2)	vmse (deg/s^2)	pmse (deg^2)	vmse (deg/s^2)
0.1			0.001	0.03	0.021	0.04
0.2	0.03	1.8	0.001	0.12	0.008	0.14
0.3	0.06	2.9	0.002	0.32	0.019	8.17
0.4	0.03	1.1	0.001	0.63	0.24	89.0
0.5			0.077	1.07	0.67	355.0
0.6	0.08	2.0	0.009	1.76	1.18	510.4
0.7	0.19	16.8	0.015	2.59	2.42	1261.0
0.8			0.018	3.88	6.36	2906.0
0.9			0.086	16.40	11.0	3942.0
1.0			0.030	6.90	12.0	4967.0

the menu selection predictor [Eqs. (3), (5), and (7)], which explains why its tracking was less accurate. The relative accuracy of the two methods in tracking a sinusoid is reflected in Table 1. At low frequencies, both predictors perform better than the human. Between 0.6 and 1 Hz, the human does better than the difference equation method, but not as well as the menu selection method. At higher frequencies, the menu selection predictor performs much better than the difference equation predictor. Because of its smaller velocity errors, we feel the menu selection predictor is more human like. We have run several other experiments to help select between the two predictors.

We favor the menu selection predictor over the difference equation predictor, because the menu selection predictor, like the human, can learn new target waveforms. Specifically, when we want it to learn a new waveform we add a new equation to its menu. The difference equation predictor was designed to track sinusoids and parabolic waveforms; it cannot learn new waveforms. (However, we are developing a difference equation predictor with adaptive coefficients that may be able to learn new waveforms.) Because the menu selection predictor can learn new waveforms, we believe that the human data are best modeled with a menu selection predictor.

Another method of comparing these two predictors involves experiments with animals. Research with monkeys suggests certain areas of the brain contain cells that respond to eye velocity (Eckmiller, 1981; Eckmiller and Mackeben, 1980). With sinusoidal target waveforms, it is difficult to differentiate between velocity cells, position cells with a time delay, and control signals such as r_c of Figs. 5 and 6. However, with our novel target waveforms, cells representing position, velocity, acceleration, or control signals could be differentiated. Such a study is being planned. Our target waveforms will be taught to a monkey, then recordings will be taken from the brain. Of course measuring signals such as U_{sp} of Fig. 2 would not help validate either the menu selection predictor or the difference equation predictor because both produce similar signals. However, measuring signals such as r_J or r_c of Fig. 2 would help to differentiate between these two predictors, because these signals are different as shown in Figs. 5 and 6. When the eye is tracking with no velocity error, r_J is equal to the output of the adaptive controller, r_c. If cells could be found with firing patterns similar to r_J in Fig. 5, then lesions of these cells should abolish zero-latency tracking of predictable waveforms. Then if human patients were found without the capability of zero-latency tracking, suggestions could be made about possible lesion sites. (In

conjunction Dr. B. Todd Troost we have recorded one patient with spinal-cerebellar degeneration that appeared to lack the capability for zero-latency tracking.)

6.2 *Limitations of the Model*

The smooth pursuit branch of our model only corrects for velocity errors. Under certain conditions static position errors can also cause slow eye movements (Wyatt and Pola, 1981; Kowler and Steinman, 1979). We investigated two ways of enlarging our model to accommodate this behavior: (1) changing the smooth pursuit branch into a position plus derivative (PD) controller, and (2) adding a low-gain, position-in position-out, pathway around the smooth pursuit branch. Only the later modification was successful. It is included in the box labeled *other inputs*.

Human open-loop tracking behavior varies from day to day and from subject. The model's behavior does not. When we first opened the loop on the model we found a saccade every 200 ms. This is not characteristic of the human so we turned off the saccadic system. Then we found that the model behavior approximated one of the human patterns described earlier. The eye position trace looked like the target position trace, except that it was larger, there was a phase lag, and there was a large time varying position offset. The phase lag of our model was larger than the phase lag of our humans, so we know that our simple model is not yet a perfect match to the human. Matching the human open-loop behavior will be the toughest challenge for future models of the smooth pursuit system.

7 Conclusions

What does this modeling teach us about the physiological system? We know that humans can overcome the 150 ms time delay of the smooth pursuit eye movement system, and track smoothly moving visual targets with zero-latency. To do the same, the model had to be able to predict target velocity and compensate for system dynamics. Therefore, we think that humans have the ability to predict, and they have internal models of their system dynamics. Because the human learns new waveforms, we think the human uses a menu selection algorithm to make the predictions.

Acknowledgements. We thank Douglas E. McHugh for providing the human data shown in Figs. 1 and 3, and Karen Bahill for editing the manuscript. Research was supported in part by National Science Foundation grant ECS-8121259.

References

Bahill, A.T.: Bioengineering: biomedical, medical and clinical engineering. Englewood Cliffs, NJ: Prentice-Hall Inc. 1981

Bahill, A.T., Brockenbrough, A.E., Troost, B.T.: Variability and development of a normative data base for saccadic eye movements. Invest. Ophthalmol. Vis. Sci. **21**, 116–125 (1981)

Bahill, A.T., Clark, M.R., Stark, L.: Dynamic overshoot in saccadic eye movements is caused by neurological control signal reversals. Exp. Neurol. **48**, 107–122 (1975)

Bahill, A.T., Latimer, J.R., Troost, B.T.: Linear homeomorphic model for human movement. IEEE Trans. Biomed. Engr. BME-**27**, 631–639 (1980)

Bahill, A.T., McDonald, J.D.: Smooth pursuit eye movements in response to predictable target motions. Vision Res. (1983) (in press)

Becker, W., Jurgens, R.: An analysis of the saccadic system by means of double step stimuli. Vision Res. **19**, 967–983 (1979)

Dallos, P.J., Jones, R.W.: Learning behavior of the eye fixation control system. IEEE Trans. Autom. Control. AC-**8**, 218–227 (1963)

Eckmiller, R.: A model of the neural network controlling foveal pursuit eye movements. In: Progress in Oculomotor Research, pp. 541–550. Fuchs, A.F., Becker, W. (eds.). New York: Elsevier/North-Holland 1981

Eckmiller, R., Mackeben, M.: Pre-motor single unit activity in the monkey brain stem correlated with eye velocity during pursuit. Brain Res. **184**, 210–214 (1980)

Greene, D.F., Ward, F.E.: Human eye tracking as a sequential input adaptive process. Biol. Cybern. **33**, 1–7 (1979)

Kleinman, D.L., Pattipati, K.R., Ephrath, A.R.: Quantifying an internal model of target motion in a manual tracking task. IEEE Syst. Man Cybern. SMC-**10**, 624–636 (1980)

Kowler, E., Steinman, R.M.: The effect of expectations on slow oculomotor control. Vision Res. **19**, 619–646 (1979)

Lanman, J., Bizzi, E., Allum, J.: The coordination of eye and head movement during smooth pursuit. Brain Res. **153**, 39–53 (1978)

Leigh, R.J., Newman, S.A., Zee, D.S., Miller, N.R.: Visual following during stimulation of an immobile eye (the open loop condition). Vision Res. **22**, 1193–1197 (1982)

Mack, A., Fendrich, R., Wong, E.: Is perceived motion a stimulus for smooth pursuit. Vision Res. **22**, 77–88 (1982)

McDonald, J.D., Bahill, A.T.: Zero-latency tracking of predictable targets by time-delay systems. Intl. J. Control. (1983) (in press)

McRuer, D.T.: Human dynamics in man-machine systems. Automatica **16**, 237–253 (1980)

Michael, J.A., Melvile Jones, G.: Dependence of visual tracking capability upon stimulus predictability. Vision Res. **6**, 707–716 (1966)

Rashbass, C.: The relationship between saccadic and smooth tracking eye movements. J. Physiol. **159**, 326–338 (1961)

Rashbass, C.: Reflexions on the control of vergence. In: Models of oculomotor behavior and control, pp. 139–148. Zuber, B.L. (ed.). Boca Raton, FL: CRC Press 1981

Robinson, D.A.: Oculomotor control signals. In: Basic mechanisms of ocular motility and their clinical implications, pp. 337–374. Lennerstrand, G., Bach-y-Rita, P. (eds.). New York: Pergamon Press 1975

Schalen, L.: Quantification of tracking eye movements in normal subjects. Acta Otolaryngol. **90**, 404–413 (1980)

Stark, L., Vossius, G., Young, L.R.: Predictive control of eye tracking movements. IRE Trans. Human Factors Electron. HFE-**3**, 52–57 (1962)

Steinbach, M.: Pursuing the perceived rather than the retinal stimulus. Vision Res. **16**, 1371–1376 (1976)

Van Gisbergen, J.A.M., Robinson, D.A., Gielen, S.: A quantitative analysis of generation of saccadic eye movements by burst neurons. J. Neurophysiol. **45**, 417–422 (1981)

Westheimer, G.: Eye movement responses to a horizontally moving visual stimulus. AMA Arch. Ophthalmol. **52**, 932–941 (1954)

Westheimer, G.: Mechanism of saccadic eye movements. AMA Arch. Ophthamol. **52**, 710–724 (1954)

Winterson, B.J., Steinman, R.M.: The effect of luminance on human smooth pursuit of perifoveal and foveal targets. Vision Res. **18**, 1165–1172 (1978)

Wyatt, H.J., Pola, J.: Slow eye movements to eccentric targets. Invest. Ophthalmol. Vis. Sci. **21**, 477–483 (1981)

Wyatt, H.J., Pola, J.: The role of perceived motion in smooth pursuit eye movements. Vision Res. **19**, 613–618 (1979)

Yasui, S., Young, L.: Perceived visual motion as effective stimulus to pursuit eye movement system. Science **190**, 906–908 (1975)

Young, L.: Pursuit eye tracking movements. In: The control of eye movements, pp. 429–443. Bach-y-Rita, P., Collins, C.C., Hyde, J. (eds.). New York: Academic Press 1971

Young, L.: Pursuit eye movements – what is being pursued. In: Control of gaze by brain stem neurons, pp. 29–36. Baker, R., Berthoz, A. (eds.). Amsterdam: Elsevier/North-Holland Biomedical Press 1977

Young, L.R.: The sampled data model and foveal dead zone for saccades. In: Models of oculomotor behavior and control, pp. 43–74. Zuber, B.L. (ed.). Boca Raton, FL: CRC Press 1981

Young, L.R., Stark, L.: Variable feedback experiments testing a sampled data model for eye tracking movements. IEEE Trans. Human Factors Electron. HFE-**4**, 38–51 (1963)

Zuber, B.L., Semmlow, J.L., Stark, L.: Frequency characteristics of the saccadic eye movement. Biophys. J. **8**, 1288–1298 (1968)

Received: July 4, 1983

Prof. A. Terry Bahill
Biomedical Engineering Program
Carnegie-Mellon University
Pittsburgh, PA 15213
USA

Verantwortlich für den Textteil: Prof. Dr. W. Reichardt, Max-Planck-Institut für biologische Kybernetik, Spemannstr. 38, D-7400 Tübingen. Verantwortlich für den Anzeigenteil: E. Lückermann, G. Sternberg, Springer-Verlag, Kurfürstendamm 237, D-1000 Berlin 15, Fernsprecher: (030)8821031, Telex: 01-85411. Springer-Verlag, Berlin·Heidelberg·New York·Tokyo.
Druck der Brühlschen Universitätsdruckerei, Gießen. Printed in Germany.

Das Heft enthält eine Beilage des Springer-Verlages Berlin Heidelberg New York Tokyo